

Sustainable and Low-cost Hydroxyapatite/Starch for the Removal of Methylene Blue from Aqueous Solutions

H. Mahroug^{a,b,*} and S. Belkaid^{b,c}

^aDepartment of Sciences and Technology, Faculty of Sciences and Technology, Tissemsilt University-38000 Tissemsilt, Algeria

^bLaboratory of Applications in Organic Electrolytes and Polyelectrolytes (LAEPO). Department of Chemistry, Faculty of Sciences, University of Tlemcen, B.P. 119, 13000, Tlemcen, Algeria

^cHigher School in Applied Sciences (ESSA)-Tlemcen, BP 165 RP Bel Horizon, Tlemcen 13000, Algeria

(Received 23 November 2022, Accepted 3 April 2023)

Hydroxyapatite/starch (HA/Star-n; « n » represents the weight ratio of HA to Star) bio-composite was obtained by using in situ chemical precipitation of calcium hydroxide using phosphoric acid in the presence of corn starch. Analysis through FTIR and XRD confirmed the formation of hydroxyapatite within the polymer matrix. To date, no work was reported in the literature concerning the use of composites based on hydroxyapatite and native starch as an adsorbent in the treatment of wastewater. For this reason, the elaborated HA/Star-n composite was used for the removal of methylene blue (MB) from the aqueous solution through batch experiments. The effect of pH (2-12); contact time (5-180 min) and dye concentration (15-100 mg l⁻¹) was explored. The results prove that the optimum pH for MB removal by the bio-composite is pH = 6. Conversely, pure HA showed minimal removal efficiency at this pH. Further, the kinetic study revealed that the adsorption of MB onto HA/Star-n is a rapid process described by the pseudo-second-order model. Results from the dye concentration study suggest that the adsorption efficiencies of the elaborated bio-composite can exceed 90% with an adsorption capacity of 45.51 mg g⁻¹ demonstrating that HA/Star-n has a great potential as an adsorbent for the removal of MB from aqueous solution.

Keywords: Hydroxyapatite, Starch, *In situ*, Methylene blue, Adsorption

INTRODUCTION

Water is an essential resource for sustaining life, yet it is often neglected and wasted in our daily activities. It is used in the majority of human and industrial activities, yet we still tend to dispose of it without much thought. With the global population increasing rapidly, the demand for water is predicted to surge in the coming decades. In addition to the water demand of the agricultural sector, there is also a significant increase in demand predicted for industries and energy production. This poses a challenge to our ability to manage and allocate this vital resource sustainably. The

INISCO World Water Assessment Program (WWAP, 2015) predicts that this issue will continue to grow, and it is crucial that we take action to address it.

Actually, the quality of the water resource is deteriorating due to the presence of pollution. The United Nations World Water Development Report (2017) has revealed that a staggering 80% of the world's wastewater is discharged back into the environment largely untreated, leading to the pollution of oceans, lakes, and rivers.

Pollution in water occurs when concentrations of substances exceed natural levels. Such pollutants can take many forms, including nutrients, microbes, heavy metals, sediments, oil, and organic chemicals. Of these, organic chemicals are a well-known type of water pollutant, which can be found in various forms such as hydrocarbons,

*Corresponding author. E-mail: mahroug.hanane@univ-tissemsilt.dz

polychlorinated biphenyls (PCBs), pesticides, and dyes [1-4]. Dyes have been recognized as a major water pollutant and have been extensively studied due to their widespread synthesis and use in various industrial sectors including paper, food, textiles, pharmaceuticals, and cosmetics. The excessive use of dyes contributes to pollution, causing many issues for both human health and aquatic systems [5]. Therefore, it is crucial to treat wastewater that contains these hazardous substances to mitigate the negative impact on the environment and human health.

Over the past few years, numerous methods and technologies have been suggested and employed for treating wastewater containing dyes. These methods include adsorption, coagulation-flocculation, oxidation, photocatalytic degradation, nanofiltration, reverse osmosis, and membrane separation [6-11]. Among these methods, adsorption is currently the most extensively used. It involves the concentration of an absorbable solute (known as adsorbate) on the surface of a solid material (*i.e.*, the adsorbent) through various forces. This approach is favored due to its simplicity, efficiency, and affordability.

In her review (2021), Maha A. Tony searched the Scopus and Google Scholar databases using the keywords "adsorption and wastewater treatment." Her findings indicate a steady increase in the number of papers related to "adsorption" each year, with over 35,000 papers in 2018 alone. The review further highlights how, over the past decade, adsorption has emerged as the most widely used method for wastewater treatment, accounting for 33% of publications on common treatment techniques [12].

Many studies have demonstrated the effectiveness of various adsorbents in the removal of different types of dyes. For instance, recent examples of adsorbents include Hydroxyapatite [13,14], grape leaves waste [15], magnetic carboxymethyl starch/poly (vinyl alcohol) composite gel [16], burnt brick pieces [17], Natural Muscovite Clay [18], Moroccan clay [19], and Polyelectrolyte [20].

Apart from the adsorption capacity, which is the amount of adsorbate (in mg) that an adsorbent (in g) can retain, several other factors significantly influence the quality and effectiveness of an adsorbent. These factors include the abundance of the adsorbent, its facility of synthesis, its low cost, its biodegradability (eco-friendly), and its ability to be regenerated [12,21,22].

Several researchers have been exploring alternative adsorbents to replace activated carbon, which is renowned for its excellent adsorption properties but is also costly to activate and reuse [21,22]. Furthermore, a range of inexpensive materials have been assessed for their ability to remove dyes, including natural adsorbents, agricultural waste, and by-products [23,24,21].

Our research aims to achieve a similar objective, which focuses on utilizing a new low-cost bio-composite material called Hydroxyapatite/Starch (HA/Star-n), where "n" represents the weight ratio of Hydroxyapatite (HA) to Starch (Star), as an adsorbent material. HA/Star-n was obtained using corn starch and the reagents of Hydroxyapatite, specifically calcium hydroxide ($\text{Ca}(\text{OH})_2$) and phosphoric acid (H_3PO_4). HA, which has the chemical formula $\text{Ca}_{10}(\text{PO}_4)_6(\text{OH})_2$, is a mineral that closely resembles to the mineral that we found in bones and teeth [25]. It can be obtained from natural sources or synthesized using various methods, including precipitation, which is the most straightforward and cost-effective method [26].

Concerning starch, it is a natural polysaccharide composed of glucose monomers linked together by 1,4 bonds. Its chemical formula is $(\text{C}_6\text{H}_{10}\text{O}_5)_n$ [27]. As shown in Fig. 1a, starch consists of two distinct polymers: amylose, which is the simpler form, and amylopectin, which is the branched form.

Our paper outlines the preparation and characterization of the HA/Star-n bio-composite material. Bio-composites obtained by combining hydroxyapatite and starch have been already reported in the literature by other researchers [28,29], but, its utilization in the environmental applications for the treatment of wastewater has not been reported so far in any paper. For this, our knowledge is devoted to the use of HA/Star-n for the removal of methylene blue (MB) cationic dye (Fig. 1b) from aqueous solution by varying different parameters that affect the adsorption which are pH, contact time and the initial concentration of the adsorbate molecules.

METHODS

Reagents

Calcium hydroxide ($\text{Ca}(\text{OH})_2$) analytical reagent was supplied by BIOCHEM Chemopharma. Phosphoric acid (H_3PO_4 at 80%) and methylene blue dye (MB, $\text{C}_{16}\text{H}_{18}\text{ClN}_3\text{S}$)

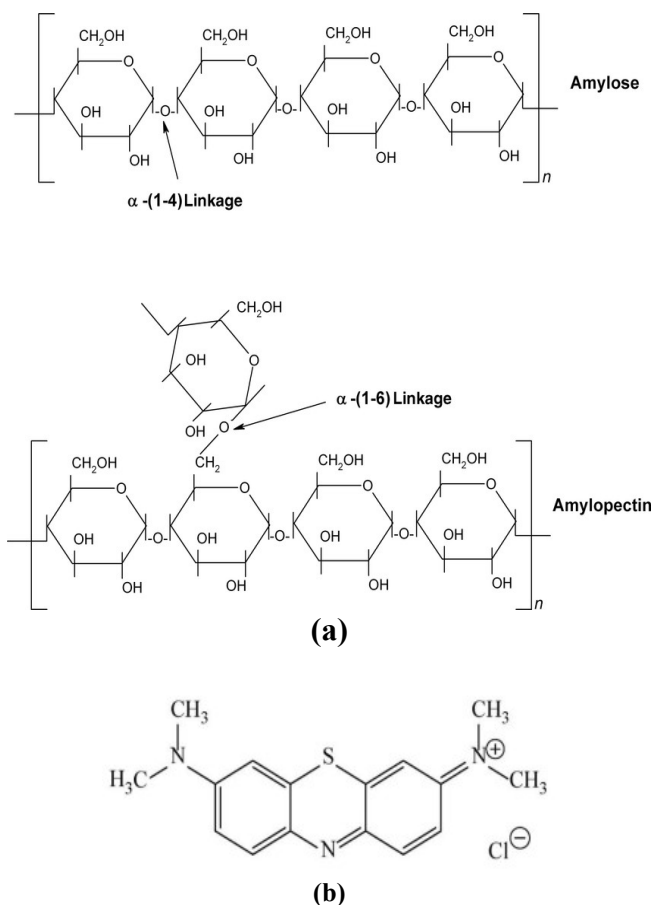


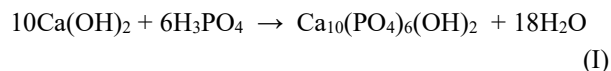
Fig. 1. Chemical structure of starch (a), MB (b).

were supplied from Sigma Aldrich Company. The used starch ((C₆H₁₀O₅)_n) was extract from corn.

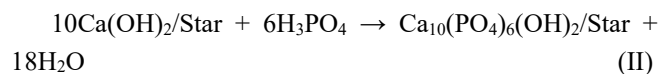
Preparation of the Adsorbents

Based on our previous works [30,14], the hydroxyapatite (HA) was prepared through a precipitation method. To formulate the HA, reaction I was followed by slowly adding phosphoric acid (H₃PO₄) drop by drop (at a rate of 2 ml min⁻¹) to a stirred aqueous suspension of calcium hydroxide (Ca(OH)₂) with a concentration of 12.5 mg l⁻¹. This suspension was prepared by dispersing 5 g of Ca(OH)₂ in 400 ml of double-distilled water, with the calcium to phosphor (Ca/P) molar ratio maintained at the stoichiometric value of 1.67. The resulting mixture was stirred at 750 rpm for 24 h at ambient temperature and normal atmospheric pressure. After 24 h, the mixture was filtered using vacuum filtration and then washed with double-distilled water before

being dried at 60 °C for 6 h.



Using the same steps and conditions as with pure HA, the HA/Star-n composite was prepared via reaction II. However, a suspension of starch in double-distilled water was first prepared, into which calcium hydroxide was added to promote the ionization of the starch's CH₂OH groups and the formation of Ca-starch complexes. Two weight ratios, "n," of HA to Star were utilized, resulting in the creation of HA/Star-1.4 and HA/Star-4 composites. Table 1 provides the quantities of the various reagents and the percentages of Starch and HA present in each powder. In this study, the amount of Ca²⁺ divalent cations is important. Consequently, we can estimate the formation of the inter-polymer complex according to Fig. 2.



The Adsorbents Characterization

The materials that were prepared underwent characterization using X-Ray Diffraction (XRD) analysis conducted by utilizing a Rigaku IV instrument with CuKα irradiation at 1.54 Å and 2 theta (2θ) set at 0.01° over a range of 20° to 70°. The purpose of the XRD was to examine the formation of HA crystals in the presence of corn starch. Additionally, Fourier Transform Infra-Red (FTIR) spectroscopy was utilized to record the infrared spectra using an Agilent Technologies Cary 600 series instrument with a resolution of 4 cm⁻¹, from 4000 cm⁻¹ to 400 cm⁻¹. Pellets were created by mixing the sample with KBr at a ratio of 1:100 (Sample/KBr), and the resulting FTIR spectra were used to identify the characteristic transmittance bands in each material.

Preparation of Methylene Blue (MB) Aqueous Solution and Adsorption Experiments

The preparation of the dye stock solution involved dissolving 500 mg of MB in one liter of double-distilled water, which was then diluted to obtain various concentrations for future use. MB solution was then mixed

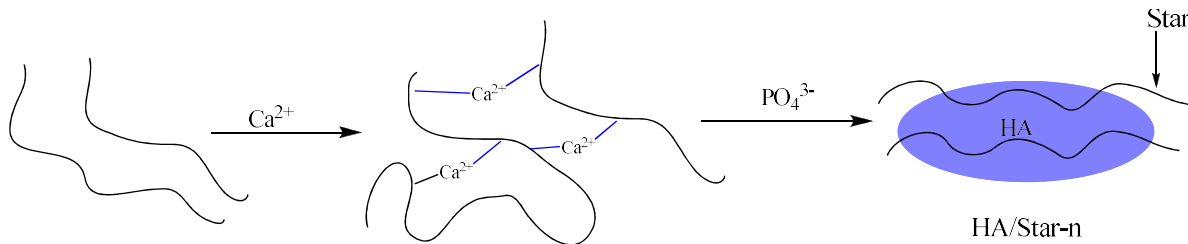


Fig. 2. In-situ formation of HA/Star-n bio-composite.

Table 1. Recapitulative Table Represents in each Elaborated Powder: the Mass of Starch m_{star} (g); the Weight Ratio between Calcium Hydroxide and Starch ($m_{Ca(OH)_2}/m_{Star}$); the Weight Ratio between Hydroxyapatite and Starch (m_{HA}/m_{Star}) Called “n”; the Percentage of HA (HA(%)) and the Percentage of Starch in each Composite (Star (%))

	m_{star} (g)	$m_{Ca(OH)_2}/m_{Star}$	$(m_{HA}/m_{Star}) = n$	HA (%)	Star (%)
HA (Ref)	0	-	-	100	0
HA/Star-1.4	5	1	1.4	57.23	42.77
HA/Star-4	1.67	3	4	80.02	19.98

with the adsorbent and stirred at 400 rpm. After a designated duration of contact time, the adsorbents were separated from the solution by means of centrifugation. The concentration of the supernatant was assessed using the UV-Vis Optizen 1412V-FB spectrophotometer, with the optimum absorption wavelength for the dye being 664 nm. q_e ($mg\ g^{-1}$) and RE (%) represents the adsorption capacity and adsorption efficiency, respectively, are calculated by means of the equations below:

$$q_e = (C_o - C_e) V/m \quad (1)$$

$$RE\ (\%) = 100 (C_o - C_e)/C_o \quad (2)$$

The values for Where “ C_o ” and “ C_e ” represent the initial and equilibrium concentrations ($mg\ l^{-1}$) of MB aqueous solution, while “ V ” represents the volume of MB solution (l) and “ m ” represents the mass (g) of the adsorbent used in each experiment.

RESULTS AND DISCUSSIONS

The Adsorbent Characterization

Figure 3 displays the characteristic bands of corn starch,

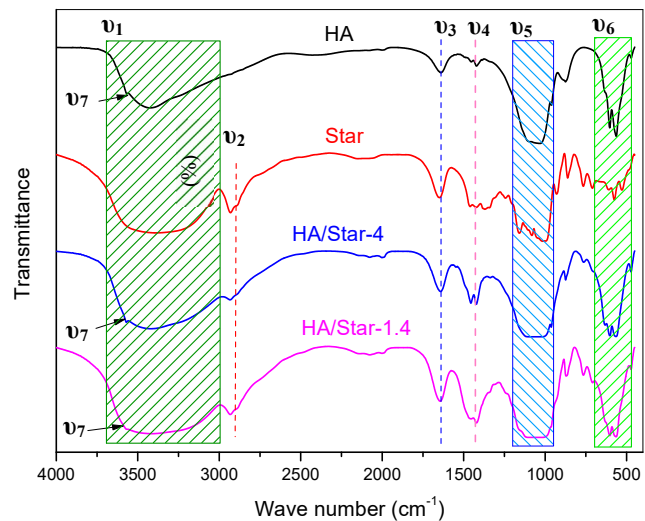


Fig. 3. FTIR spectra of HA, Star, and HA/Star-n.

pure HA, and the two bio-composites. In the native starch, a broad band from $2990\ cm^{-1}$ to $3668\ cm^{-1}$ (ν_1) indicates the stretching mode of OH groups. Stretching vibration of the C-H bond is represented by the double bands at $2943\ cm^{-1}$ and $2905\ cm^{-1}$ (ν_2) [28,29], whereas the presence of intermolecular hydrogen bonds is confirmed by the band at

1658 cm^{-1} (ν_3). The transmittance bands from 1340 cm^{-1} to 1468 cm^{-1} (ν_4) are attributed to the symmetric deformation of CH_2 groups and asymmetric stretching of C-H bonds [31]. The C-O vibration is identified by the band at 1161 cm^{-1} (ν_5), indicating the existence of B-configuration [28]. The strong band located at 935 cm^{-1} (region of ν_5) is attributed to the C-O-C bond of anhydroglucose units (AGU) [29].

The FTIR spectrum of HA confirms the formation of calcium phosphate through the presence of bands at 1100 cm^{-1} (ν_5) and 554 cm^{-1} (ν_6) assigned to the phosphate groups. The bending mode of adsorbed water in the hydroxyapatite structure is represented by the small band at 1632 cm^{-1} (ν_3) [32,33]. The broad envelope observed between 2632 cm^{-1} and 3706 cm^{-1} (ν_1) indicates the O-H stretching vibration of adsorbed water and the O-H stretching vibration of the hydroxyapatite. The stretching mode of O-H groups at the surface of HA crystals is identified by the very small peak at 3568 cm^{-1} (ν_7). Furthermore, the presence of carbonated hydroxyapatite is confirmed by the bands at 1419 cm^{-1} and 1457 cm^{-1} (ν_4) [34].

Concerning the HA/Star-n, its spectra contain both the bands attributed to the HA structure and bands attributed to the polymer part with a slight shift in the position of bands indicating the interaction between the polymer and the HA crystals, *i.e.* the formation of the bio-composite.

Figure 4 shows XRD diffractograms indicating the presence of peaks centered at 26°, 32°, 40°, 50° and 64°, which are characteristic of the carbonated hydroxyapatite structure according to the PDF card no 01-072-9863. The presence of the same diffraction peaks in the two composites allows us to deduce that starch does not have a negative effect on the formation of hydroxyapatite. Despite the significant amount of starch in the two composites, the intensity of the peaks is similar in all three diffractograms. This can be attributed to a balance between the quantity of the mineral phase and the level of crystallinity in each composite.

Methylene Blue Dye Removal

Effect of pH. Numerous studies have shown that pH is a critical parameter in the adsorption process, as it affects both the functional groups of the adsorbent and the adsorbate. In this study, the removal of MB dye by HA, Star, and HA/Star-n was investigated by varying the pH of the MB aqueous solution from 2 to 12 using HCl (1 M) and NaOH (1 M).

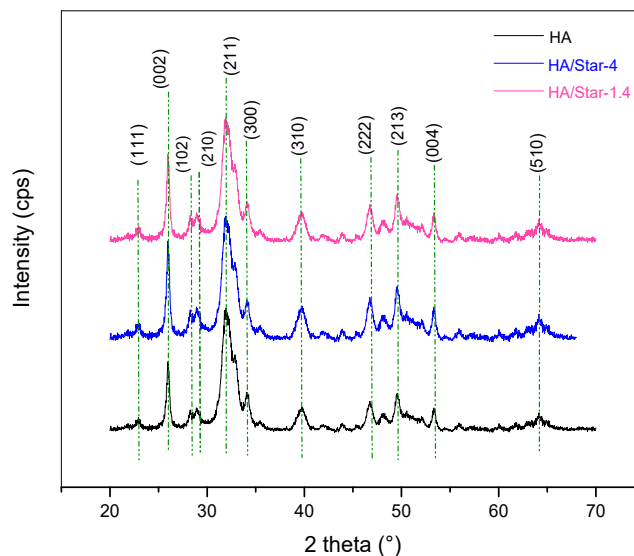


Fig. 4. XRD patterns of HA and HA/Star-n.

Figure 5 illustrates that the curve representing the retention efficiency of MB by HA is divided into two distinct parts. In the first part, the hydroxyapatite shows a decrease in retention efficiency (RE(%)) from 55.81% to 22.39% up to pH 6. In the second part, the retention efficiency starts increasing and reaches 91.34% at pH 12. This behaviour can be attributed to the presence of a positive charge in the MB molecules. At a lower pH, the HA surface becomes positively charged through protonation reaction with H^+ , which does not attract the positively charged MB molecules. As the solution pH increases, the HA surface undergoes deprotonation reaction, giving it a negative charge that interacts easily with the positive charge of MB molecules. Similar phenomena have been observed in other recently reported studies [28,35]. In the case of starch, the retention efficiency (RE (%)) increases significantly with increasing pH up to pH 10, as shown in Fig. 6. However, the increase in pH from pH 10 to pH 12 has little effect on RE (%), which decreases from 73.26% to 70.1%.

For the HA/Star-n bio-composite, the retention efficiency (RE (%)) curves can be divided into three distinct parts. The first part, ranging from pH 2 to pH 6, shows a significant increase in RE (%) for both HA/Star-1.4 and HA/Star-4. In For the HA/Star-n bio-composite, the retention efficiency (RE (%)) curves can be divided into three distinct parts. The first part, ranging from pH 2 to pH 6, shows a significant

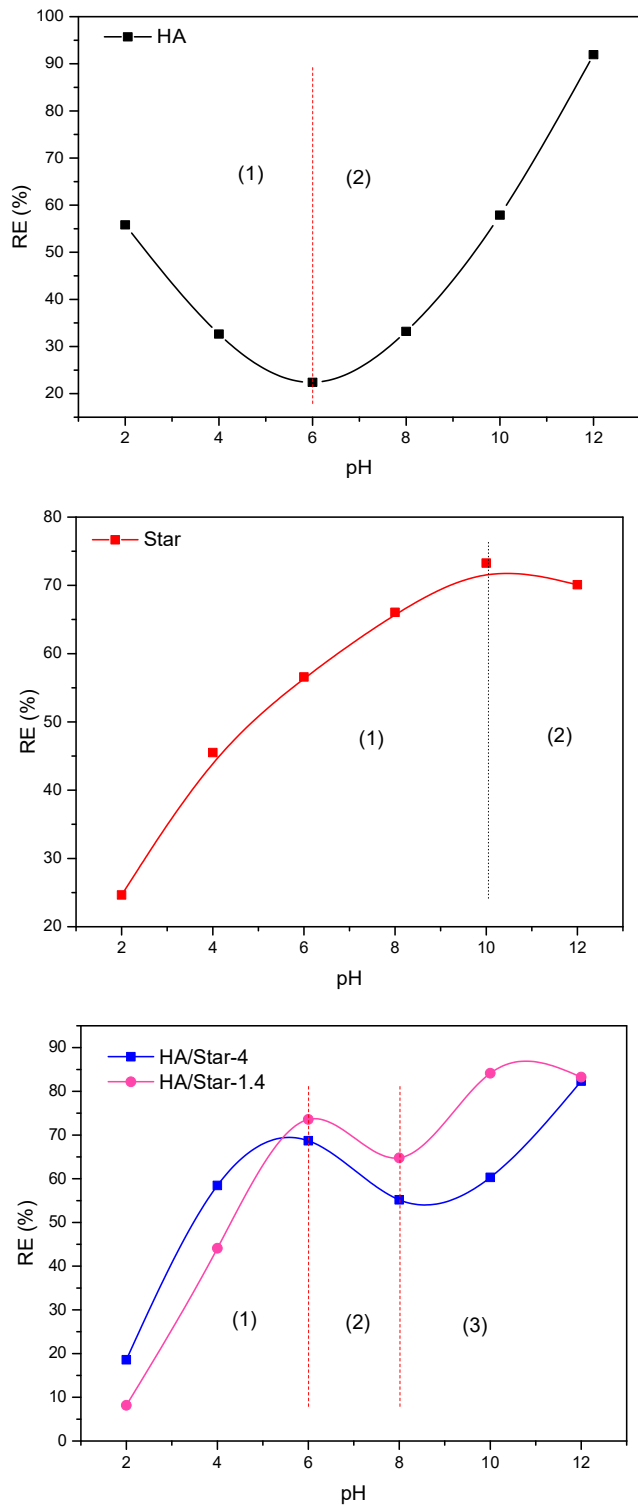


Fig. 5. MB adsorption efficiency *versus* pH for HA, Star, and HA/Star-n. [MB] = 10 mg l⁻¹, V_{MB} = 40 mg l⁻¹, m_{ads} = 25 mg, t = 3 h, T = 20 °C, 400 rpm.

increase in RE (%) for both HA/Star-1.4 and HA/Star-4. In the second region, from pH 6 to pH 8, a slight decrease in RE (%) is observed. However, as shown in the same figure, from pH 8, RE (%) begins to increase again, and reaches 82.34% and 83.24% for HA/Star-4 and HA/Star-1.4, respectively.

By comparison, the results indicate that HA/Star-4 and HA/Star-1.4 exhibit behavior similar to that of native corn starch in the pH range of 2-6 and 8-12. Therefore, it can be deduced that starch is the primary component of HA/Star-n that plays a crucial role in MB retention. In fact, HA/Star-n has an intrinsic behaviour that corresponds to a decrease in RE (%) when the pH rises from 6 to 8. However, in the same pH range, the curves presented in Fig. 5 clearly show an increase in retention efficiency (RE (%)) when the pure phases (HA and native starch) were used separately.

Figure 5 also reveals that the minimum value of RE (22.39 %) is achieved at pH 6 when hydroxyapatite was used as adsorbent material. At the same pH, the RE is higher and equals 56.58% when MB is removed using corn starch. However, when the bio-composite is used for MB retention, the retention efficiency is significantly improved. The values obtained are 68.69% and 73.59% for HA/Star-4 and HA/Star-1.4, respectively. As a result, the effect of contact time and MB concentration was carried out at pH 6 using the composite HA/Star-n.

Effect of contact time. Figure 6 depicts the impact of contact time on the adsorption efficiency. In these experiments, 40 mg of HA/Star-n was added to 40 ml of MB solution with a concentration of 20 mg l⁻¹. The adsorption process can be divided into two distinct phases, with the first phase lasting 140 min. During this phase, MB is fixed onto the surface of the adsorbents and diffuses into the pores of the bio-composites, which can be observed through different series of adsorption followed by partial desorption of MB molecules for both adsorbents. It is noteworthy that the highest RE (%) is achieved after 30 min of contact between the MB aqueous solution and HA/Star-4, while the maximum is observed at 60 min for the composite HA/Star-1.4.

After 140 min of the adsorbent and adsorbate being in contact, the adsorption of MB reached a plateau in the second phase, indicating that the equilibrium had been attained. The presence of the plateau means that the adsorption of MB reached the equilibrium under the experimental conditions considered and means also that the rate of adsorption is

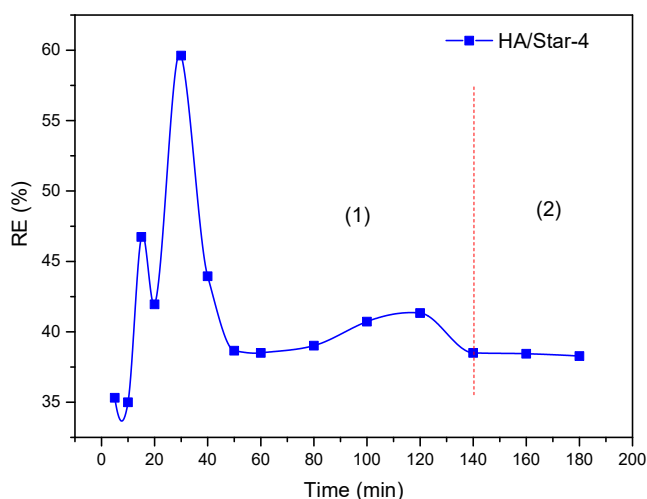
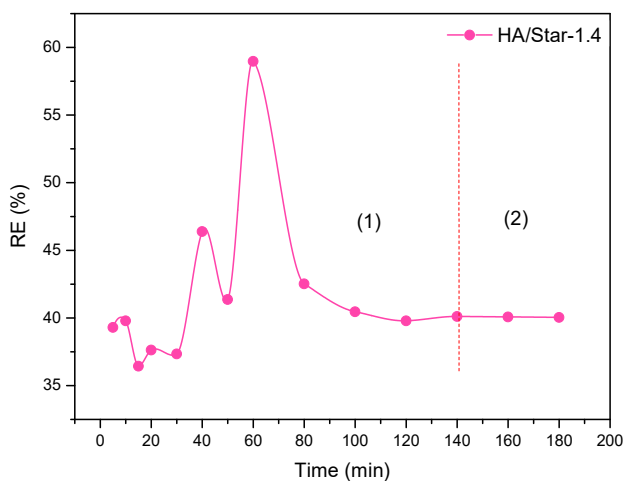


Fig. 6. Time-dependent RE (%) of MB removed by HA/Star-n. [MB] = 20 mg l⁻¹, V_{MB} = 40 mg l⁻¹, m_{ads} = 40 mg, pH = 6, T = 20 °C, 400 rpm.

balanced by the rate of desorption. As a result, a contact time of 3 h was established as the equilibrium contact time for the remainder of the study.

The experimental data were fitted by means of the pseudo-second-order model given by Eq. (3).

$$\text{Pseudo-second order equation: } \frac{t}{q_t} = \frac{1}{Kq_e^2} + \frac{1}{q_e}t \quad (3)$$

K (g mg⁻¹ min⁻¹) is the rate constant and q_e (mg g⁻¹) is the

adsorption capacity at equilibrium. These constants were determined from the slopes and intercepts of the lines obtained by plotting t/q_t against t.

The graphical representations of this model are given in Fig. 7. The correlation coefficient (R²) suggests that the adsorption of MB for both adsorbents is described by the pseudo-second-order model, indicating a multi-stage adsorption process. Thus, the adsorption rate is dependent on the number of active sites in the adsorbent material. This finding aligns with previous studies that also found the adsorption of methylene blue onto various composites-based hydroxyapatite to follow the pseudo-second-order model [36-39].

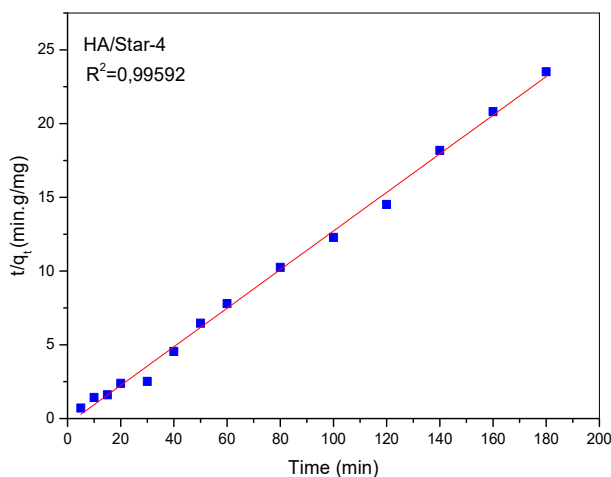
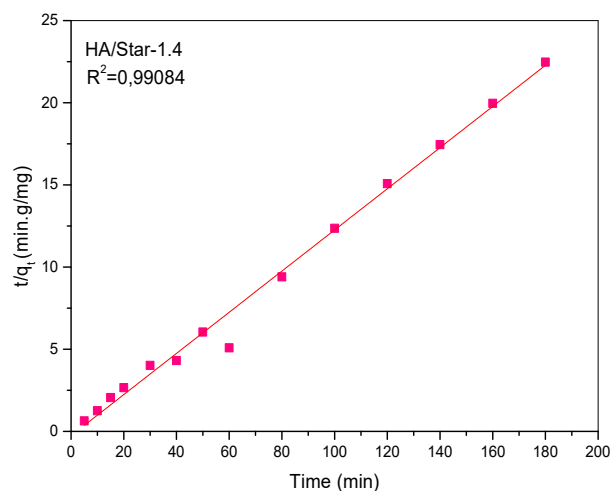


Fig. 7. Linear fit of MB adsorption experimental data obtained by using pseudo-second-order model.

Table 2 presents the characteristic parameters obtained from Fig. 7. Notably, the adsorption capacities (q_e) calculated from the pseudo-second-order model align with the experimental adsorption capacities (q_e (exp)) observed after 140 min of contact between the adsorbent and adsorbate.

Effect of MB initial concentration. The effect of the initial dye concentration was studied under the same pH and contact time as previously explored, with concentrations ranging from 15 mg l⁻¹ to 100 mg l⁻¹. As illustrated in Fig. 8, the quantity of MB adsorbed onto HA/Star-n (q_e) increased as the initial dye concentration (C_0) rose, peaking at 50 mg l⁻¹ for HA/Star-1.4 and 40 mg l⁻¹ for HA/Star-4. This resulted in an adsorption capacity of 45.51 mg g⁻¹ for HA/Star-1.4 with a removal efficiency (RE) of 90.80%, and an adsorption capacity of 23.53 mg g⁻¹ for HA/Star-4 with a RE of 57.95%.

When the initial dye concentration (C_0) increases to more significant concentrations of 50 mg l⁻¹ to 150 mg l⁻¹, it becomes evident that both the adsorption capacity (q_e) and efficiency (RE) decrease. This is mainly due to the substantial interactions between the adsorbate molecules, in comparison to the interactions that exist between the adsorbate (MB) and the adsorbent (HA/Star-n). Several authors also explain that the decrease in q_e as the C_0 of dye rises is due to the excess in dye molecules, which causes a longer contact time between the active sites of the adsorbent and the adsorbate molecules [38,40,41].

Based on the existing literature, it is important to note that unmodified hydroxyapatite is not a suitable candidate for retaining MB, as per our previous work and other studies [28, 42]. However, in the current study, HA/Star-1.4 is identified as the most effective adsorbent. Table 3 shows that its adsorption capacity is superior to other adsorbents reported in various studies [42-48].

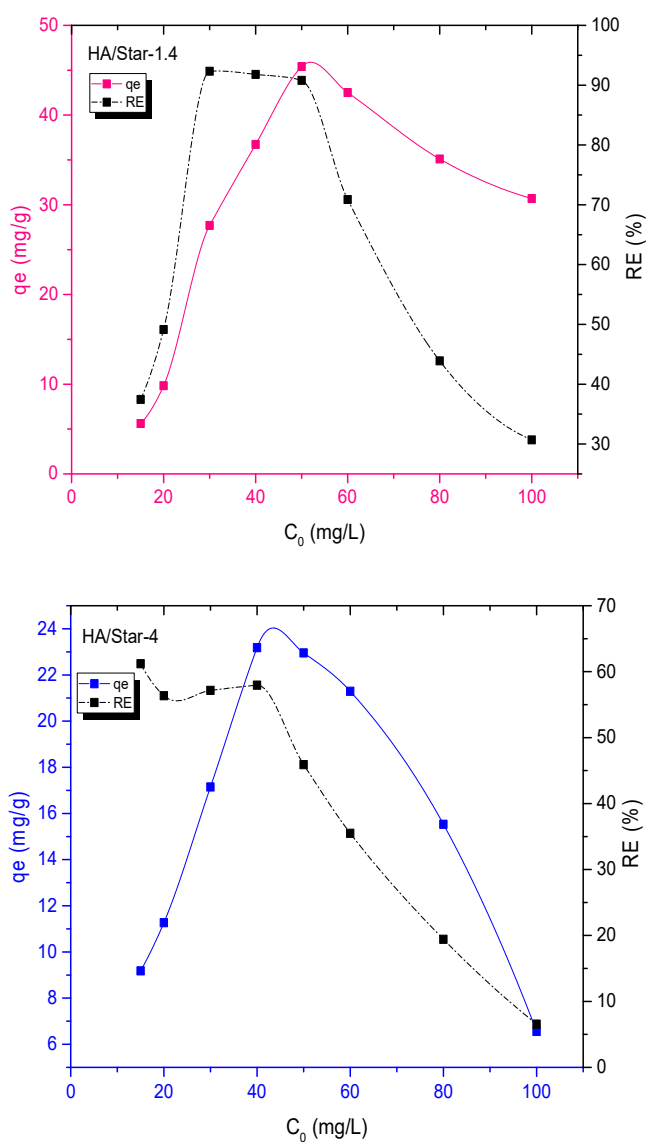


Fig. 8. MB removal capacity (q_e) and MB removal efficiency (RE) as a function of the initial dye concentration, $V_{MB} = 40$ mg l⁻¹, $m_{ads} = 40$ mg, pH = 6, T = 20 °C, $t_{eq} = 3$ h, 400 rpm.

Table 2. Characteristic Parameters Obtained by the Pseudo-second-order Model

HA/Star-1.4				HA/Star-4			
q_e (exp) (mg g ⁻¹)	q_e (mg g ⁻¹)	K_1 (min ⁻¹)	R^2	q_e (exp) (mg g ⁻¹)	q_e (mg g ⁻¹)	K_1 (min ⁻¹)	R^2
9.824	7.984	-0.059	0.991	11.267	7.641	-0.047	0.995

Table 3. Maximal Adsorption Capacity q_{\max} (mg g^{-1}) for MB Removal by Different Materials

Material	q_{\max} (mg g^{-1})	Ref.
HA	0	[42]
Fly ash	3.074	[43]
HAP: Bentonite mix	20.70	[44]
Clay	6.3	[45]
Black Tea Wastes	3	[46]
Zeolite ZK	21.41	[47]
SDBS-modified ZSM-5	15.68	
Hydroxysodalite	10.82	
Crosslinked porous starch	9.46	[48]
HA/Star-4	23.53	This work
HA/Star-1.4	45.51	

CONCLUSION

Based on the findings of the current study, it can be inferred that HA/Star-n shows great potential as an adsorbent for removing MB dye from aqueous solutions, particularly due to its simple preparation method. Moreover, its constituent phases, hydroxyapatite and corn starch, are non-toxic and possess eco-friendly properties. The formation of the composite was confirmed through FTIR analysis, and the presence of crystalline hydroxyapatite within the polymer chains was demonstrated using XRD patterns. The experiments for batch adsorption were conducted while monitoring pH, contact time, and MB concentration. From the study on the effect of pH on MB uptake, it was deduced that the optimum pH for MB removal is 6, as it is close to the natural pH of the MB aqueous solution. The kinetic study showed that MB adsorption by HA/Star-n is a rapid process that follows the pseudo-second-order kinetic model. The study on the effect of initial dye concentration revealed that both materials exhibited significant adsorption capacities, with values of 23.53 mg g^{-1} (RE = 57.95%) and 45.51 mg g^{-1} (RE = 90.80%) for HA/Star-4 and HA/Star-1.4, respectively.

ACKNOWLEDGMENT

We would like to thank the General Directorate for

Scientific Research and Technological Development in Algeria for their financial support.

REFERENCES

- [1] Thilagam, H.; Gopalakrishnan, S., Environmental Deterioration Due to Existing and Emerging Persistent Organic Pollutants: An Overview. In: Vasanthi, M., Sivasankar, V., Sunitha, T.G. (eds) Organic pollutants. Emerging Contaminants and Associated Treatment Technologies. Springer, Cham 2022, DOI: 10.1007/978-3-030-72441-2_3.
- [2] Ahila, K. G.; Vinodini, S. K.; Ancy Jenifer, A.; Thamaraiselvi, C., An Overview on Eco-friendly Remediation of Toxic Organic Contaminants from Textile Dyeing Industry Wastewater. In: Vasanthi, M., Sivasankar, V., Sunitha, T.G. (eds) Organic pollutants. Emerging Contaminants and Associated Treatment Technologies. Springer, Cham 2022, DOI: 10.1007/978-3-030-72441-2_17.
- [3] Asadi, T.; Najafi, P.; Chavoshi, E.; Hoodaji, M., Effect of hydrocarbonic pollutants on the stability and soil water repellency intensity: A case study in Bandar Abbas Oil Refinery, Hormozgan province. *Iran. Environ. Health Eng. Manag.* **2022**, *9*, 105-113, DOI: 10.34172/EHEM.2022.12.
- [4] Saleh, I. A.; Zouari, N.; Al-Ghouti, M. A., Removal of pesticides from water and wastewater: Chemical, physical and biological treatment approaches. *Environ. Technol. Innov.* **2020**, *19*, 2352-1864, DOI: 10.1016/j.eti.2020.101026.
- [5] Gong, G.; Zhang, F.; Cheng, Z.; Zhou, L., Facile fabrication of magnetic carboxymethyl starch/poly(vinyl alcohol) composite gel for methylene blue removal. *Int. J. Biol. Macromol.* **2015**, *81*, 205-211. DOI: 10.1016/j.ijbiomac.2015.07.061.
- [6] Gadekar, M. R.; Ahammed, M. M., Coagulation/flocculation process for dye removal using water treatment residuals: modelling through artificial neural networks. *Desalination. Water Treat.* **2016**, *57*, 26392-26400. DOI: 10.1080/19443994.2016.1165150.
- [7] Dwijenra, N. K. A.; Patra, I.; Ansari, M. J.; Saadoon, N.; Al Mashhadani, Z. I.; Obaid, N. H.; Sivaraman, R.; Alawsi, T.; Jabbar, A. H.; Mustafa, Y. F.,

- Insights into the Electronic Properties of Coumarins: A Comparative Study Synthesis and Characterization of Fe₂O₃/Mn₂O₃ Magnetic Nanocomposites for the Photocatalytic Degradation of Methylene Blue. *Phys. Chem. Res.* **2023**, *11*, 437-447, DOI: 10.22036/PCR.2022.336018.2070.
- [8] Kadhim, R. J.; Al-Ani, F. H.; Al-shaeli Muayad, Alsally, Q. F.; Figoli, A., Removal of Dyes Using Graphene Oxide (GO) Mixed Matrix Membranes. *Membranes.* **2020**, *10*, 366. DOI: 10.3390/membranes10120366.
- [9] Pai, S.; Kini, M. S.; Selvaraj, R., A review on adsorptive removal of dyes from wastewater by hydroxyapatite nanocomposites. *Environ. Sci. Pollut. Res.* **2021**, *28*, 11835-11849, DOI: 10.1007/s11356-019-07319-9.
- [10] Adel Niaei, H.; Rostamizadeh, M.; Maasumi, F.; Darabi, J., Kinetic, Isotherm, and Thermodynamic Studies of Methylene Blue Adsorption over Metal-doped Zeolite Nano-adsorbent. *Phys. Chem. Res.* **2021**, *9*, 17-30, DOI: 10.22036/PCR.2020.233844.1781.
- [11] Kulasoorya, T. P. K.; Priyantha, N.; Navaratne, A. N., Removal of textile dyes from industrial effluents using burnt brick pieces: adsorption isotherms, kinetics and desorption. *SN Appl. Sci.* **2020**, *2*, 1789, DOI: 10.1007/s42452-020-03533-0.
- [12] Tony, M. A., Low-cost adsorbents for environmental pollution control: a concise systematic review from the prospective of principles, mechanism and their applications. *J. Dispers. Sci. Technol.* **2021**, *43*, 1612-1633, DOI: 10.1080/01932691.2021.1878037.
- [13] Sricharoen, P.; Kongsri, S.; Kukusamude, C.; Areerob, Y.; Nuengmatcha, P.; Chanthai, S.; Limchoowong, N., Ultrasound-irradiated synthesis of 3-mercaptopropyl trimethoxysilane-modified hydroxyapatite derived from fish-scale residues followed by ultrasound-assisted organic dyes removal. *Sci. Rep.* **2021**, *11*, 5560, DOI: 10.1038/s41598-021-85206-5.
- [14] Mahroug, H., Kinetic, Isotherm and Thermodynamic Study of Acid Blue 29 Textile Dye Removal from Aqueous Solution by Using Hydroxyapatite and Partially Hydrolyzed Polyacrylamide Modified Hydroxyapatite; *Russ. J. Phys. Chem. A.* **2021**, *95*, 2558-2566, DOI: 10.1134/S0036024421130136.
- [15] Mousavi, S. A.; Mahmoudi, A.; Amiri, S.; Darvishi, P.; Noori, E., Methylene blue removal using grape leaves waste: optimization and modeling. *Appl. Water. Sci.* **2022**, *12*, 112-123. DOI: 10.1007/s13201-022-01648-w.
- [16] Gong, G.; Zhang, F.; Cheng, Z.; Zhou, L., Facile fabrication of magnetic carboxymethyl starch/poly(vinyl alcohol) composite gel for methylene blue removal. *Int. J. Biol. Macromol.* **2015**, *81*, 205-211, DOI: 10.1016/j.ijbiomac.2015.07.061.
- [17] Moosavi, S.; Lai, C. W.; Gan, S.; Zamiri, G., Akbarzadeh Pivehzhani, O.; Johan, M. R., Application of Efficient Magnetic Particles and Activated Carbon for Dye Removal from Wastewater. *ACS Omega.* **2020**, *5*, 20684-20697, DOI: 10.1021/acsomega.0c01905.
- [18] Amrhar, O., Berisha, A., El Gana, L., Nassali, H., S. Elyoubi, M., Removal of methylene blue dye by adsorption onto Natural Muscovite Clay: experimental, theoretical and computational investigation. *Int. J. Environ. Anal. Chem.* **2021**, *1-26*, DOI: 10.1080/03067319.2021.1897119.
- [19] Elmoubarki, R.; Mahjoubi, F. Z.; Tounsadi, H.; Moustadraf, J.; Abdennouri, M.; Zouhri, A.; El-Albani, A.; Barka, N., Adsorption of textile dyes on raw and decanted Moroccan clays: Kinetics, equilibrium and thermodynamics. *Water Resour. Ind.* **2015**, *9*, 16-29, DOI: 10.1016/j.wri.2014.11.001.
- [20] Herrera-González, A. M.; Peláez-Cid, A. A., Adsorption of textile dyes present in aqueous solution and wastewater using polyelectrolytes derived from chitosan. *J. Chem. Technol. Biotechnol.* **2017**, *92*, 1488-1495, DOI: 10.1002/jctb.5214.
- [21] Bharathi, K. S.; Ramesh, S. T., Removal of dyes using agricultural waste as low-cost adsorbents: a review. *Appl. water sci.* **2013**, *3*, 773-790, DOI: 10.1007/s13201-013-0117-y.
- [22] Gupta, V. K., Suhas., Application of low-cost adsorbents for dye removal-A review. *J. Environ. Manage.* **2009**, *90*, 2313-2342, DOI: 10.1016/j.jenvman.2008.11.017.
- [23] Mishra, S.; Cheng, L.; Maiti, A., The utilization of agro-biomass/by products for effective bio-removal of dyes from dyeing wastewater: A comprehensive review. *J. Environ. Chem. Eng.* **2021**, *9*, 104901, DOI: 10.1016/j.jece.2020.104901.

- [24] Al-Kadhi, N. S., Removal of Fluorescein Dye from Aqueous Solutions Using Natural and Chemically Treated Pine Sawdust. *Int. J. Anal. Chem.* **2020**, 8824368, DOI: 10.1155/2020/8824368.
- [25] Chen, L.; Al-Bayatee, S.; Khurshid, Z.; Shavandi, A.; Brunton, P.; Ratnayake, J., Hydroxyapatite in Oral Care Products- A Review. *Materials.* **2021**, *14*, 4865, DOI: 10.3390/ma14174865.
- [26] Haider, S.; Han, S. S.; Kang, I. -K., Recent advances in the synthesis, functionalization and biomedical applications of hydroxyapatite: a review. *RSC. Adv.* **2017**, *7*, 7442-7458, DOI: 10.1039/c6ra26124h.
- [27] Magallanes-Cruz, P. A.; Flores-Silva, P. C.; Bello-Perez, L. A., Starch Structure Influences Its Digestibility: A Review. *J. Food Sci.* **2017**, *82*, 2016-2023, DOI: 10.1111/1750-3841.13809.
- [28] Pramanik, S.; Agarwala, P.; Vasudevan, K.; Sarkar, K., Human-lymphocyte cell friendly starch-hydroxyapatite biodegradable composites: Hydrophilic mechanism, mechanical, and structural impact. *J. Appl. Polym. Sci.* **2020**, *137*, 48913, DOI: 10.1002/app.48913.
- [29] Koski, C.; Onuiké, B.; Bandyopadhyay, A.; Bose, S., Starch-Hydroxyapatite Composite Bone Scaffold Fabrication Utilizing a Slurry Extrusion-Based Solid Freeform Fabricator. *Addit. Manuf.* **2018**, *24*, 47-59, DOI: 10.1016/j.addma.2018.08.030.
- [30] Mansri, A.; Mahroug, H.; Dergal, F., In situ preparation of hydroxyapatite composites into hydrolysed polyacrylamide solution and methylene blue dye retention. *Turk. J. Chem.* **2019**, *43*, 213-228, DOI: 10.3906/kim-1803-49.
- [31] Abdullah, A. H. D.; Chalimah, S.; Primadona, I.; Hanantyo, M. H. G., Physical and chemical properties of corn, cassava, and potato starches. *IOP Conf. Ser.: Earth Environ. Sci.* **2018**, *160*, 012003, DOI: 10.1088/1755-1315/160/1/012003.
- [32] Varma, H. K.; Babu, S. S., Synthesis of calcium phosphate bioceramics by citrate gel pyrolysis method. *Ceram. Int.* **2005**, *31*, 109-114, DOI: 10.1016/j.ceramint.2004.03.041.
- [33] Castro, M. A. M.; Portela, T. O.; Correa, G. S.; Oliveira, M. M.; Rangel, J. H. G.; Rodrigues, S. F.; Mercury, J. M. R., Synthesis of hydroxyapatite by hydrothermal and microwave irradiation methods from biogenic calcium source varying pH and synthesis time. *Bol. Soc. Esp. Ceram. Vidr.* **2020**, *61*, 35-41, DOI: 10.1016/j.bsecv.2020.06.003.
- [34] Mahroug, H.; Mansri, A.; Dergal, F., The effect of calcium suspension concentration on the hydroxyapatite structures and purity. *Rev. Roum. Chim.* **2019**, *64*, 277-286, DOI: 10.33224/rch/2019.64.3.10.
- [35] Akartasse, N.; Azzaoui, K.; Mejdoubi, E.; Hammouti, B.; Elansari, L. L.; Abou-salama, M.; Aaddouz, M.; Sabbahi, R.; Rhazi, L.; Siaj, M., Environmental-Friendly Adsorbent Composite Based on Hydroxyapatite/ Hydroxypropyl Methyl-Cellulose for Removal of Cationic Dyes from an Aqueous Solution. *Polymers.* **2022**, *14*, 2147. DOI: 10.3390/polym14112147.
- [36] Oun, A. A.; Kamal, K. H.; Farroh, K.; Ali, E. F.; Hassan, M. A., Development of fast and high-efficiency sponge-gourd fibers (*Luffa cylindrica*)/hydroxyapatite composites for removal of lead and methylene blue. *Arab. J. Chem.* **2021**, *14*, 103281, DOI: 10.1016/j.arabjc.2021.103281.
- [37] Agougui, H.; Jabli, M.; Majdoub, H., Synthesis, characterization of hydroxyapatite-lambda carrageenan, and evaluation of its performance for the adsorption of methylene blue from aqueous suspension. *J. Appl. Polym. Sci.* **2017**, *134*, 45385, DOI: 10.1002/app.45385.
- [38] Sharma, K.; Sharma, S.; Sharma, V.; Mishra, P. K.; Ekielski, A.; Sharma, V.; Kumar, V., Methylene Blue Dye Adsorption from Wastewater Using Hydroxyapatite/Gold Nanocomposite: Kinetic and Thermodynamics Studies. *Nanomaterials.* **2021**, *11*, 1403, DOI: 10.3390/nano11061403.
- [39] Sricharoen, P.; Kongsri, S.; Kukulamude, C.; Areerob, Y.; Nuengmatcha, P.; Chanthai, S.; Limchoowong, N., Ultrasound-irradiated synthesis of 3-mercaptopropyl trimethoxysilane-modified hydroxyapatite derived from fish-scale residues followed by ultrasound-assisted organic dyes removal. *Sci Rep.* **2021**, *11*, 5560, DOI: 10.1038/s41598-021-85206-5.
- [40] Adeogun, A. I.; Ofudje, E. A.; Idowu, M. A.; Kareem, S. O.; Vahidhabanu, S.; Babu, B. R., Biowaste-Derived

- Hydroxyapatite for Effective Removal of Reactive Yellow 4 Dye: Equilibrium, Kinetic, and Thermodynamic Studies. *ACS Omega*. **2018**, 3, 1991-2000, DOI: 10.1021/acsomega.7b01768.
- [41] Ferreira dos Santos, C.; Gomes, P. S.; Almeida, M. M.; Willinger, M. -G.; Franke, R. -P.; Fernandes, M. H.; Costa, M. E., Gold-dotted hydroxyapatite nanoparticles as multifunctional platforms for medical applications. *RSC Adv.* **2015**, 5, 69184-69195, DOI: 10.1039/c5ra11978b.
- [42] Li, C.; Ge, X.; Liu, S.; Liu, F., Synthesis of Novel Core-Shell Structured Hydroxyapatite/Meso-Silica for Removal of Methylene Blue from Aqueous Solutions. *Adv. Mater. Res.* **2012**, 543, 463-464, DOI: 10.4028/www.scientific.net/amr.463-464.543.
- [43] Basava Rao, V. V.; Mohan Rao, S. R., Adsorption studies on treatment of textile dyeing industrial effluent by flyash, *Chem. Eng. J.* **2006**, 116, 77-84, DOI: 10.1016/j.cej.2005.09.029.
- [44] Annan, E.; Arkorful, G. K.; Konadu, D. S.; Asimeng, B.; Dodoo-Arhin, D.; Egblewogbe, M., Synthesis and Characterization of Hydroxyapatite- (HAP-) Clay Composites and Adsorption Studies on Methylene Blue for Water Treatment. *J. Chem.* **2021**, 2021, 3833737, DOI: 10.1155/2021/3833737.
- [45] Mukherjee, K.; Kedia, A.; Jagajjanani Rao, K.; Dhir, S.; Paria, S., Adsorption enhancement of methylene blue dye at kaolinite clay-water interface influenced by electrolyte solutions. *RSC Adv.* **2015**, 5, 30654-30659, DOI: 10.1039/C5RA03534A.
- [46] Ullah, A.; Zahoor, M.; Ud Din, W.; Muhammad, M.; Ali Khan, F.; Sohail, A.; Ullah, R.; Ali, E. A.; Ananda Murthy, H. C., Removal of Methylene Blue from Aqueous Solution Using Black Tea Wastes: Used as Efficient Adsorbent. *Adsorpt. Sci. Technol.* **2022**, 2022, 5713077, DOI: 10.1155/2022/5713077.
- [47] EL-Mekkawi, D. M.; Ibrahim, F. A.; Selim, M. M., Removal of methylene blue from water using zeolites prepared from Egyptian kaolins collected from different sources. *J. Environ. Chem. Eng.* **2016**, 4, 1417-1422, DOI: 10.1016/j.jece.2016.01.007.
- [48] Guo, L.; Li, G.; Liu, J.; Meng, Y.; Tang, Y., Adsorptive decolorization of methylene blue by crosslinked porous starch. *Carbohydr. Polym.* **2013**, 93, 374-379, DOI: 10.1016/j.carbpol.2012.12.019.